

High Reynolds Number Separated Flow Solutions Using Navier-Stokes and Approximate Equations

M. Napolitano*

Università degli Studi di Bari, Bari, Italy

The present study is concerned with the numerical simulation of high Reynolds number, two-dimensional, incompressible, steady, weakly separated laminar flows. It is shown that a "well-designed" code can solve the complete Navier-Stokes equations and the parabolized vorticity equations with the same convergence rate, so that solving the full Navier-Stokes equations is recommended when dealing with a new problem. Furthermore, the boundary-layer equations in vorticity/stream-function form are solved without encountering the Goldstein singularity at separation. Finally, for a typical high Reynolds number weakly separated flow, it is shown that, in the presence of a non-negligible skewness in the body-oriented computational grid, the parabolized vorticity approximation still provides very reliable solutions, whereas an interacting boundary-layer model provides results plagued with severe errors.

Introduction

HIGH Reynolds number (Re) attached flows have been computed routinely for several decades using the classical boundary-layer (BL) theory of Prandtl: the inviscid flow past the body of interest is computed first and then the BL equations are solved, using the inviscid pressure gradient as a datum, to evaluate the skin friction and thus the aerodynamic drag. Eventually, the displacement thickness obtained by the BL equations is added to the body to provide an "augmented body" around which the inviscid flow is recomputed, and so on, as stipulated by a rigorous asymptotic expansion theory provided by Van Dyke.¹ Unfortunately, the classical BL theory breaks down in the presence of flow separation, so that a lot of computational effort has been devoted to the development of numerical methods for solving the Navier-Stokes (NS) equations. However, theoretical studies (see, e.g., Ref. 2) as well as numerical investigations (see, e.g., Refs. 3 and 4) have shown that, for high Re weakly separated flows, the terms contained in the classical BL equations are sufficient to model the flowfield even in the separation region. It is now understood that the failure of the classical BL theory when the pressure gradient is prescribed is due to the lack of the upstream propagation required to account for the "elliptic" character of the separation phenomenon; in fact, solutions to the BL equations, which are regular through the separation point, have been obtained by prescribing either the displacement thickness⁵ or the wall shear⁶ in place of the pressure gradient.

More generally, useful solutions for high Re separated flows can be obtained from an appropriate subset of the NS equations, provided that the strong viscous-inviscid interaction phenomenon is correctly accounted for. Among the many approximate equations used in the literature, the most widely employed and investigated appear to be the so-called thin-layer Navier-Stokes (TLNS) and interacting boundary-layer (IBL) equations (see, e.g., Ref. 7). Starting from the NS equations written in a body-oriented orthogonal coordinate system, the TLNS equations are easily obtained by dropping the viscous terms in the streamwise direction. The

IBL equations are obtained by coupling the classical BL equations with a pressure interaction law that accounts for the variations in the inviscid (outer) pressure field induced by the viscous effects. The TLNS equations can then be considered, from an asymptotic point of view, as a composite set of equations uniformly valid in both the inner (viscous) and the outer (inviscid) regions. The IBL equations are valid only in the viscous region, whereas the inviscid flow is computed by means of another set of equations with the viscous-inviscid interaction phenomenon being accounted for iteratively; for instance, the inviscid and viscous flows are computed using the same displacement thickness and the calculation is repeated until both sets of equations provide the same pressure distribution along the augmented body. For the case of the vorticity/stream-function of interest here, the approximate model corresponding to the TLNS equations is obtained simply by dropping the streamwise diffusion term in the vorticity equation, so as to provide the so-called parabolized vorticity (PV) equations.^{3,4} The classical BL equations are obtained by also dropping the streamwise derivatives in the stream function equation, according to the asymptotic order-of-magnitude analysis of Prandtl. Finally, the IBL equations are obtained by coupling the BL equations in the viscous region to the Laplace equation for the stream function in the inviscid region, so as to allow for the viscous-inviscid interaction.

To date, a large number of numerical studies have shown that for many flowfields of practical interest (namely, for high Re weakly separated flows), the PV or even the IBL equations provide a satisfactory answer, so that it would appear to be an unnecessary waste of computational effort to resort to the complete NS equations (see, e.g., Refs. 8–11). Furthermore, thanks to the theoretical work of Smith and Cheng,^{12–14} it begins to appear more and more evident that the IBL equations are capable of also predicting the massive separation phenomenon and stall.

Nevertheless, the NS equations still remain the only numerical tool capable of verifying the correctness of the new asymptotic theories. Furthermore, a well-designed NS code for computing high Re , weakly separated flows has to be very similar in nature to efficient PV or IBL codes; i.e., it has to account implicitly for downstream propagation and transversal-viscous effects and iteratively for the upstream influence. Such a code will experience the same convergence rate (see, e.g., Ref. 11) when computing the terms present only in the PV or IBL equations or retaining all of the terms in the complete NS equations. The extra computational cost

Presented as Paper 85-1688 at the AIAA 18th Fluid Dynamics, Plasmadynamics and Lasers Conference, Cincinnati, OH, July 16–18, 1985; received Oct. 24, 1985; revision received May 5, 1986. Copyright © American Institute of Aeronautics and Astronautics, Inc., 1985. All rights reserved.

*Professor, Istituto di Macchine. Member AIAA.

required to evaluate the negligible streamwise diffusion terms will be insignificant with respect to that required to solve the PV or the IBL equations, and certainly worth paying if one of these terms turns out to be essential to model a locally important phenomenon. It is to be pointed out that many IBL codes solve only the BL equations in the viscous region, with the pressure/displacement interaction law computed according to a thin-airfoil theory. Admittedly, these methods may require significantly less computational effort than codes solving the complete NS equations, especially for the case of supersonic outer flow.

The aim of this work is to demonstrate that, for high Re weakly separated flows, a well-designed NS-PV code can solve the NS or PV equations with exactly the same convergence rate and at about the same computational cost. Therefore, when solving a new problem, the additional cost of retaining all of the NS terms is minimal and justified by the fact that the model employed certainly includes all of the physically relevant phenomena. Of course, by no means is it implied that solving the NS equations by "brute force" is an appropriate investigating tool! Asymptotic analyses are essential to prescribe the appropriate computational grids that capture the different length scales and the location and type of the far-field boundary conditions, as well as to validate the numerical solutions.

Furthermore, the present study will demonstrate that, for high Re weakly separated flows, solutions can be obtained to the vorticity/stream-function BL equations that are regular through the separation point. In particular, for the case of the flow in a symmetric channel with a smooth expansion proposed by Roache¹⁵—a nearly parallel flow with negligible streamwise curvature effects—these solutions of the BL equations will be shown to be in very good agreement with results of the PV and the complete NS equations.

Finally, for a typical high Re weakly separated flow, already studied by several authors,⁸⁻¹¹ it is shown that PV-type equations still provide results in good agreement with the complete NS solutions in the presence of non-negligible skewness of the body-fitted coordinate system, whereas IBL-type equations experience marked errors due to the incorrect representation of the streamwise pressure gradient.

Governing Equations and Numerical Technique

The steady-state vorticity/stream-function equations are given in a system of body-oriented curvilinear coordinates as

$$(\psi_\eta \omega_\xi - \psi_\xi \omega_\eta)/J - (\alpha \omega_{\xi\xi} - 2\beta \omega_{\xi\eta} + \gamma \omega_{\eta\eta} + \sigma \omega_\eta + \tau \omega_\xi)/Re = 0 \quad (1)$$

$$\alpha \psi_{\xi\xi} - 2\beta \psi_{\xi\eta} + \gamma \psi_{\eta\eta} + \sigma \psi_\eta + \tau \psi_\xi + \omega = 0 \quad (2)$$

where ω is the vorticity, ψ the stream function, ξ and η the streamwise and transversal coordinates, J , α , β , γ , σ , and τ the Jacobian and scale factors of the mapping of the physical coordinates x and y into the computational coordinates ξ and η , and the subscripts indicate the partial derivatives.¹⁶ Furthermore, the underlined terms are to be dropped to obtain the PV equations and those in boldface are the additional terms that must be dropped to obtain the classical BL equations. Of course, BL theory strictly requires the use of orthogonal coordinates, for which β in Eqs. (1) and (2) is identically zero. However, the PV equations have been shown to be valid also in a "mildly nonorthogonal coordinate system,"¹¹ so that the aforementioned definition of PV and BL equations is used here. With the vorticity term eliminated, Eq. (2) is obviously the Laplace equation for the stream function governing the inviscid irrotational portion of the flowfield.

In the present study, the incremental block-line-Gauss-Seidel method proposed in Ref. 17 is used as an efficient numerical tool for iteratively solving Eqs. (1) and (2). The governing equation are first parabolized in time¹⁸ and then

discretized and linearized using a two-level implicit Euler scheme and the delta approach of Beam and Warming¹⁹ to give

$$\begin{aligned} \Delta\omega/\Delta t + (\psi_\eta^n \Delta\omega_\xi + \omega_\xi^n \Delta\psi_\eta - \psi_\xi^n \Delta\omega_\eta - \omega_\eta^n \Delta\psi_\xi)/J \\ - (\alpha \Delta\omega_{\xi\xi} + \gamma \Delta\omega_{\eta\eta} + \sigma \Delta\omega_\eta + \tau \Delta\omega_\xi)/Re \\ = - [(\psi_\eta^n \omega_\xi^n) - (\psi_\xi^n \omega_\eta^n)]/J \\ + (\alpha \omega_{\xi\xi}^n - 2\beta \omega_{\xi\eta}^n + \gamma \omega_{\eta\eta}^n + \sigma \omega_\eta^n + \tau \omega_\xi^n)/Re \end{aligned} \quad (3)$$

$$\begin{aligned} \Delta\psi/\Delta t - \alpha \Delta\psi_{\xi\xi} - \gamma \Delta\psi_{\eta\eta} - \sigma \Delta\psi_\eta - \tau \Delta\psi_\xi - \Delta\omega \\ = \alpha \psi_{\xi\xi}^n - 2\beta \psi_{\xi\eta}^n + \gamma \psi_{\eta\eta}^n + \sigma \psi_\eta^n + \tau \psi_\xi^n + \omega^n \end{aligned} \quad (4)$$

where Δt is the time step [which can be different in Eqs. (3) and (4) and can also vary at every iteration], $\Delta\omega = \omega^{n+1} - \omega^n$, the superscripts n and $n+1$ indicate the old and new time levels, t^n and $t^{n+1} = t^n + \Delta t$, etc. Notice that the mixed derivatives are evaluated at the old time level t^n (i.e., explicitly) and therefore do not appear in delta form. The presence of such terms in the vorticity equation of the complete NS equations (when a nonorthogonal computational grid is employed) can be critical insofar as they may reduce the stability and therefore the convergence rate of the numerical method.

Equations (3) and (4) are then discretized in space using second-order-accurate central differences throughout, except for all of the incremental convective terms of the vorticity equation in the left side of Eq. (3), which are approximated using first-order-accurate upwind differences, and solved by a line Gauss-Seidel relaxation method marching in the main direction of the flow (see Ref. 17 for details). It is noteworthy that, by using such a deferred correction strategy for the advection terms in the vorticity equation, upstream propagation is allowed, although explicitly, even when solving the BL equations, i.e., when all the streamwise elliptic terms are dropped from the equations. Also, the final solution enjoys the accuracy of the central differences and of the conservative form and the linear system to be solved along each vertical line is diagonally dominant. The solution is finally updated as $(\omega^n, \psi^n) \rightarrow (\omega^n, \psi^n) + (\Delta\omega, \Delta\psi)$ and the process is repeated until a satisfactory convergence criterion is met.

Results

The first problem considered in this study is the weakly separated channel flow proposed by Roache.¹⁵ The geometry of the channel, together with the appropriate boundary conditions and the orthogonal 41×21 grid employed in this study is given in Fig. 1 for the case $Re = 10$. Roache has shown that, if the length of the channel is increased proportionally to Re , for $Re \gg 1$ the solution takes on a quasi-self-similar form, i.e., the skin friction at the wall becomes independent of Re when plotted vs x/Re . As such, the present problem is very suitable to assess the capability of a numerical technique to compute high Re weakly separated flows. More importantly, for $Re \gg 1$, the length of the separation bubble is found to increase proportionally to Re , whereas its height remains constant, so that, from an order of magnitude analysis, it can be argued that

$$u = \mathcal{O}(1) \quad (5)$$

$$v = \mathcal{O}(1/Re) \quad (6)$$

$$\partial/\partial y = \mathcal{O}(1) \quad (7)$$

$$\partial/\partial x = \mathcal{O}(1/Re) \quad (8)$$

where $\mathcal{O}(\)$ indicates the standard asymptotic order-of-magnitude symbol. If, for large values of Re , Eqs. (5-8) are

true, than the PV equations and even the BL equations should provide results practically coincident with those computed using the complete NS equations. The same code was therefore used to solve the three aforementioned sets of equations, for the case $Re=10^6$, using the 41×21 mesh depicted in Fig. 1. The results for the vorticity at the wall were found to be identical (to machine accuracy, i.e., six significant digits), with no indication of the singularity at separation appearing when solving the BL equations. In order to better assess this last very important issue, as well as the accuracy of the present numerical results, a grid refinement study was conducted in both the x (quasistreamwise) and y (quasinormal) directions, using meshes with 61×21 , 81×21 , 41×41 , and 41×61 grid points, the horizontal mesh size being always uniform and the normal one increasing at a constant rate equal to 1.1, starting from the wall. The results of the mesh refinement studies are given in Figs. 2 and 3 as the vorticity distributions along the wall: it clearly appears that the basic 41×21 mesh solution is already "exact" to plotting accuracy. Again, the NS, PV, and BL results coincided to machine accuracy for all cases and no indication of singularity at separation was ever encountered.

It is noteworthy that, the length of the channel being equal to $Re/3$, the longitudinal step size is always several orders of magnitude larger than the order-one BL thickness, so that also an "ill-posed" marching method could possibly recover the correct solution¹⁵ by swamping out all branching solutions, due to truncation errors. Therefore, the $Re=100$ flow case was also considered in this study: the BL equations were solved using two meshes having 81×21 and 161×21 grid

points. The two solutions were found to coincide with each other and (after proper scaling) with those of Figs. 2 and 3 to plotting accuracy. In conclusion, the BL equations, when solved in an iterative way that allows for upstream propagation, clearly do not encounter any singularity at the separation point. This result is not surprising insofar as the value of the stream function is prescribed as a boundary condition at the centerline of the channel; such a condition is equivalent to prescribing the displacement thickness in the pressure-velocity BL equations, which has been shown to produce separated flow solutions that are regular through the separation point.⁵ Finally, the convergence rate for all three sets of equations and the same mesh was always found to be identical. In Fig. 4, the average variation of the vorticity between two successive iterations is plotted vs the iteration number for five different meshes. The convergence rate of the method is remarkable and just about independent of the mesh employed for the calculations; this last result is very atypical of any relaxation method, so that it is most likely due to the quasi-one-dimensional (parallel) nature of the flow.

In order to compare the present NS and PV solvers for an "extreme" situation, the $Re=10$ flow was also considered. For such a case, the geometry is considerably distorted (see Fig. 1) and the Reynolds number is very low, so that it is reasonable to expect large differences between the NS and the PV solutions, whereas the BL equations are obviously meaningless. However, the present NS and PV solutions still provide wall vorticity distributions that are qualitatively very similar. (See Fig. 5.) This result provides further evidence of the broad range of applicability of the PV equations.

In all the above calculations, an appropriate Couette flow was used at every longitudinal location as the initial condition. The time step was chosen equal to Re and then updated after every iteration, dividing its initial value by the vorticity error. Therefore, for the particular case $Re=10^6$, the time steps were so large that the time derivatives played no role in the computational process.

In order to compare the NS and PV solutions for a more general (less parallel) flow and in the presence of local skewness of the computational grid, as well as to assess the efficiency of the present code with respect to several high Re weakly separated flow solvers,⁸⁻¹¹ a second well-known high Re weakly separated flow problem was considered in the present study; namely, the plane flow in a symmetric diffuser. The nondimensional semiheight of the diffuser is equal to 1, the Reynolds number (defined with respect to such a reference

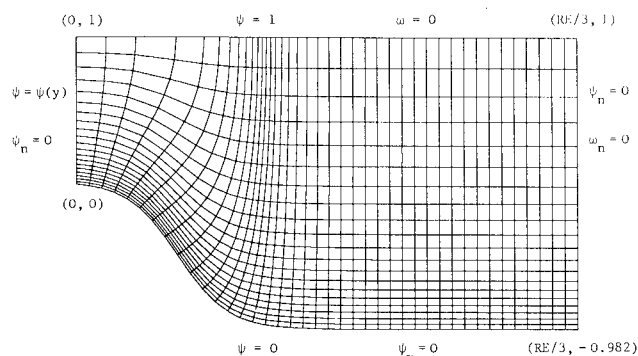


Fig. 1 Channel flow geometry, computational grid, and boundary conditions.

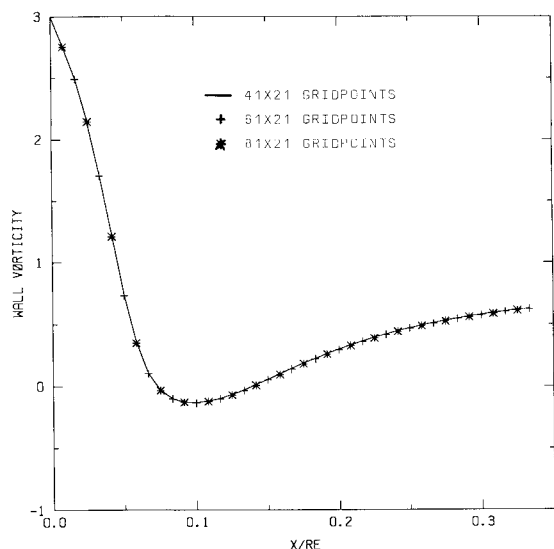


Fig. 2 Longitudinal mesh refinement study for channel flow at $Re=10^6$.

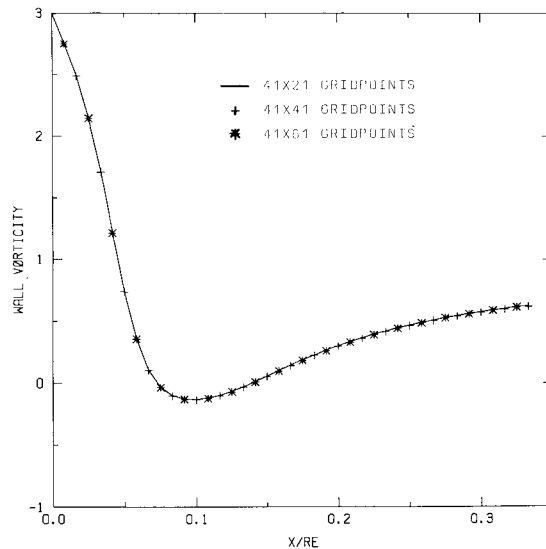


Fig. 3 Transversal mesh refinement study for channel flow at $Re=10^6$.

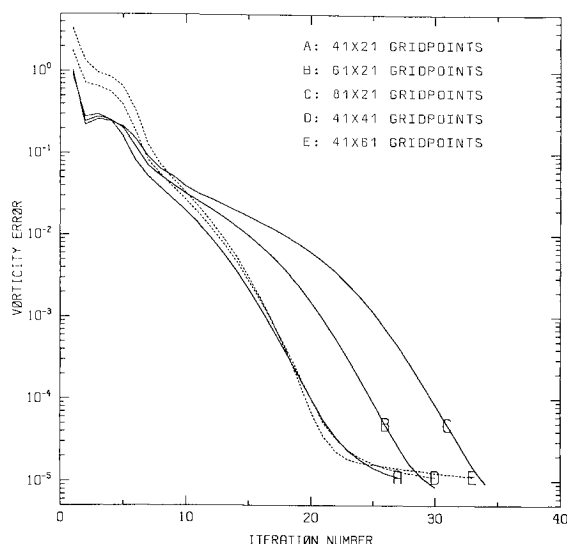


Fig. 4 Convergence histories for channel flow at $Re = 10^6$.

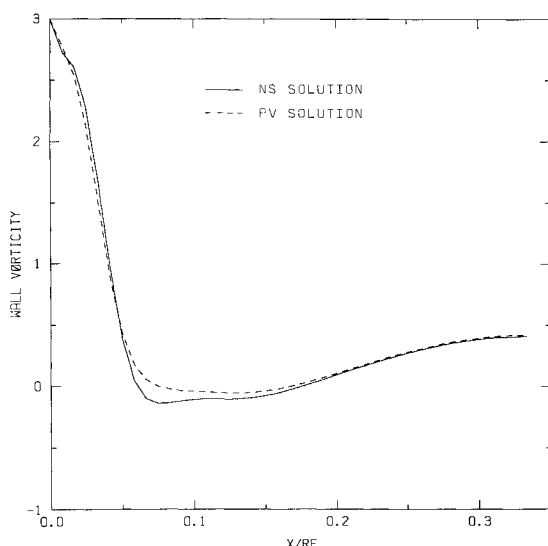


Fig. 5 Comparison of NS and PV results for channel flow at $Re = 10$.

length and to a unit velocity) is equal to 6250, and the inlet flow is a Blasius boundary layer produced by a flat plate whose leading edge is two units before the entrance of the diffuser; also, the midplane is located at $y = 1$, whereas the (bottom) wall $y_w(x)$ is defined as follows:

$$\begin{aligned} y_w(x) &= 0 & \text{for } -1 < x < 0 \\ &= A[x^2(3-2x)] & \text{for } 0 \leq x \leq 1 \\ &= A & \text{for } 1 < x < x_{\text{out}} \end{aligned} \quad (9)$$

Two flow cases were considered, with $A = -0.08$, $x_{\text{out}} = 3$ and $A = -0.16$, $x_{\text{out}} = 6$. The computational meshes employed in this study contain 81 and 71 equally spaced gridpoints in the x direction for the first and second flow cases, respectively, and always 41 grid points in the y direction, stretched in such a way that the vertical mesh size grows at a constant rate of 1.08 starting from the wall. See Fig. 6 where the geometry and the computational grid for the second flow case is depicted. For the first problem, the 81×41 grid was chosen fine enough to provide reasonably accurate answers to compare with previously published results. For the second

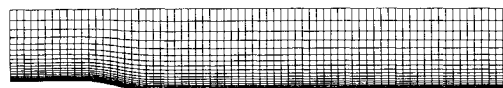


Fig. 6 Geometry and computational grid for diffuser flow with $A = -0.16$.

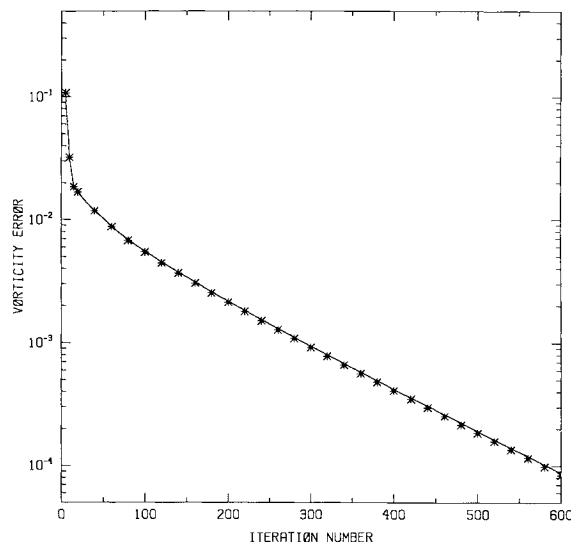


Fig. 7 Convergence history for diffuser flow with $A = -0.08$.

problem, the 71×41 grid of Fig. 6 is not considered adequate to provide accurate solutions, but valuable to provide a meaningful one-to-one comparison between NS and PV results obtained using the same numerical method and mesh. In the range $0 < x < 1$, the mesh is nonorthogonal, so that the mixed derivatives in Eqs. (1-4) may be expected to play a considerable role, especially for the second more severe flow situation. For both flow cases, results were obtained using the same computer code to solve the NS and the PV equations. The initial condition was taken to be the inlet boundary condition in the entire flowfield. Symmetry was enforced by prescribing the value of the stream function at the center of the diffuser ($y = 1$), where a zero vorticity was also prescribed. At the wall, the standard no-slip, zero-injection conditions were imposed and, finally, the BL equations were solved at the outlet station, with the first derivatives evaluated as three-point second-order-accurate backward differences. The time steps at the first iteration were taken to be equal to 0.1 for the vorticity equation and 1000 for the stream-function equation. After every iteration, the time steps were adjusted by dividing the initial values by the average deltas for the vorticity and stream function, respectively. An over-relaxation factor⁸ of 1.5 was also used for the stream-function equation only ($\psi^n - \psi^n + 1.5\Delta\psi$). These values were the first and only ones used, i.e., no optimization of the convergence rate of the method was pursued. For the first flow case, IBL-type equations were also solved by also dropping the streamwise derivatives in the stream-function equation in the viscous region, while retaining them in the outer inviscid flow (namely, in the upper half of the computational grid points), where a Laplace equation for the stream function was thus solved, the vorticity being vanishingly small.

The results are given in Figs. 7 and 8, which show the convergence histories of the NS (solid lines) and PV (symbols) equations for the two flow cases, and in Figs. 9 and 10, where the corresponding wall vorticity (shear) distributions are depicted. For the first flow case, the wall shear predicted by the IBL-type equations is also shown as a broken line. From the results in Figs. 7-10, the following conclusions

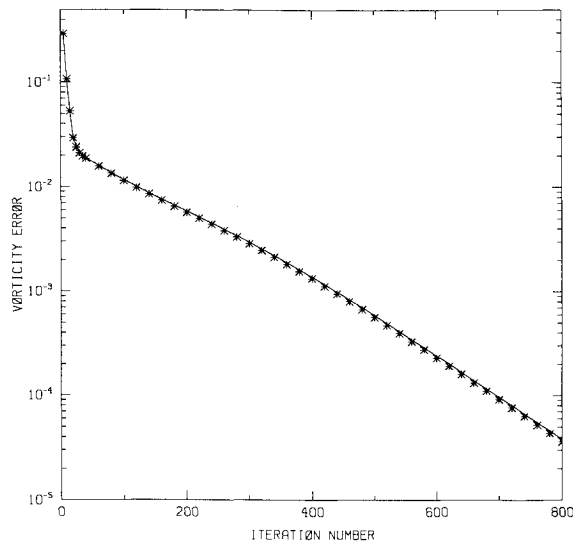


Fig. 8 Convergence history for diffuser flow with $A = -0.16$.

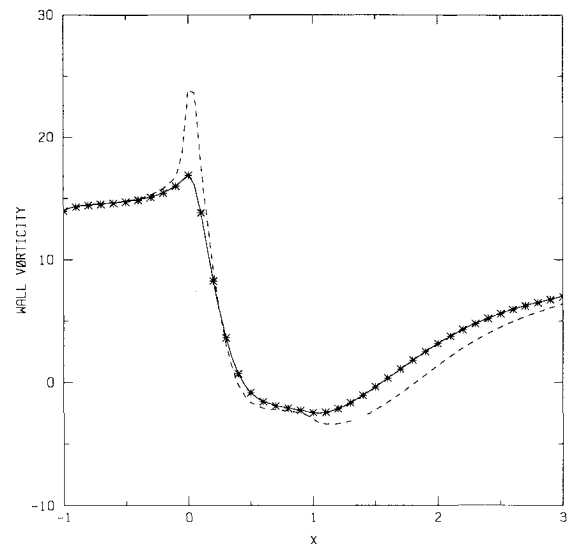


Fig. 9 Wall vorticity results for diffuser flow with $A = -0.08$.

emerge. The NS and PV equations provide practically identical results and convergence rate. The IBL-type equations are plagued, instead, with local errors near the curvature discontinuities at the wall, where the pressure gradient induced by the inviscid turning of the streamlines is not accounted for correctly. In this respect, it is remarkable that, for the second flow case, the IBL-type equations still converge without difficulties, but the final solution is completely destroyed by spatial oscillations produced by the more severe curvature discontinuities. Also, the convergence rate of the IBL-type equations (not reported in Figs. 7 and 8) is slightly slower than that of the NS and PV equations due to the local larger gradients to be computed.

The present solution given in Fig. 9, after proper scaling, is found to be in reasonable agreement with those of Edwards and Carter⁸ and of Hoffman,¹¹ but predicts a slightly longer separation region. The PV equations were therefore solved using a finer 121×61 mesh; the results practically coincide with those obtained using the coarser 81×41 mesh. The solutions of Fig. 9 are thus considered "correct," to plotting accuracy, and the slight discrepancy with the aforementioned solutions is believed to be due to their first-order accuracy in the streamwise direction. For the second flow case, Refs. 8 and 11 do not report the skin-friction distribution. However, the length and position of the separated region can be compared using the streamlines plot of Ref. 8. Again, the present solutions predict a separation region longer than that computed by Edwards and Carter,⁸ but in this case the present results are not considered accurate because the 71×41 mesh of Fig. 6 is not sufficiently fine and because the outlet boundary conditions are not imposed sufficiently far downstream. An important point needs attention: the solutions of Ref. 8 use a correct IBL model that contains the same terms retained in the present IBL-type approximation, when an appropriate, orthogonal grid is employed. Therefore, for the problem at hand, the normal pressure gradient is indeed negligible in the (separated) boundary layer, but the present IBL-type model cannot be accurate insofar as it neglects the pressure gradient in the y direction, which is considerably inclined with respect to the direction normal to the wall in the range $0 < x < 1$. In conclusion, the PV equations can still be used in the presence of mild skewness of the computational mesh, but the IBL equations strictly require a body-oriented coordinate grid that is orthogonal, at least near the body surface.

As far as the efficiency of the calculations is concerned, the approach employed in this study seems to require from two to four times more iterations than other current PV or

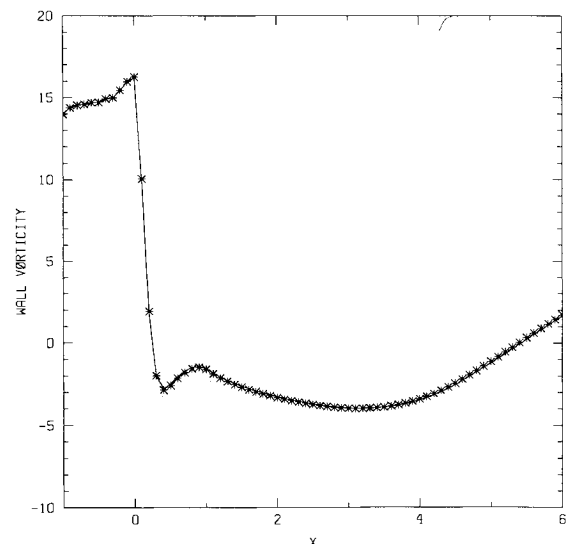


Fig. 10 Wall vorticity results for diffuser flow with $A = -0.16$.

IBL solvers.⁸⁻¹¹ On the other hand, it turns out to be extremely robust, since no parameter was ever optimized or changed when solving the second more difficult problem, for which no substantial deterioration of the convergence rate was encountered. (See Figs. 7 and 8.) Furthermore, the present method does not resort to any kind of inner iteration, so that a global iteration for the 81×41 grid requires only 3.3 s of CPU time on a HP 9000/9050 minicomputer, and effectively employs second-order-accurate central differences for all of the first derivatives, so that it is anticipated to be more accurate (for an equivalent mesh) than methods resorting to first-order-accurate upwind differences⁹ or to the FLARE approximation in the separated region.⁸ Anyway, efficiency is not considered a major issue, because the aim of this work was by no means to provide the "most efficient" high Re weakly separated flow solver, but to demonstrate that the NS and PV equations can be solved with essentially the same efficiency, so that it is preferable to retain all of the terms in the complete NS equations in order to avoid unpleasant "surprises." In this respect, it is felt that such a goal has been achieved, together with the secondary ones of obtaining separated flow solutions to the BL equations, without encountering the separation singularity, and of assessing the in-

fluence of skewness in the computational mesh on the performance of PV- and IBL-type models.

Acknowledgments

This work was supported by ONR Grant N00014-82-K-0184 while the author was in residence at Yale University, Research Center for Scientific Computation, by the Ministero Pubblica Istruzione and by the Consiglio Nazionale Ricerche. The author is indebted to Drs. M. J. Werle, D. E. Edwards, J. E. Carter, and M. Hafez and Profs. R. T. Davis and L. Quartapelle for many helpful suggestions and interesting discussions and to the referees for their very valuable comments.

References

- ¹Van Dyke, M., *Perturbation Methods in Fluid Mechanics*, Parabolic Press, Stanford, CA, 1975.
- ²Stewartson, K., "Multistructured Boundary Layers on Flat Plates and Related Bodies," *Advances in Applied Mechanics*, Vol. 14, 1974, p. 145.
- ³Ghia, K. N., Ghia, U., and Tesch, W. A., "Evaluation of Several Approximate Models for Laminar Incompressible Separation by Comparison with Complete Navier-Stokes Solutions," AGARD CP 168, 1975, p. 6-1.
- ⁴Werle, M. J. and Bernstein, J. M., "A Comparative Numerical Study for Models of the Navier-Stokes Equations for Incompressible Separated Flows," AIAA Paper 75-48, 1975.
- ⁵Catherall, D. and Mangler, K., "The Integration of the Two Dimensional Boundary-Layer Equations Past a Point of Vanishing Skin Friction," *Journal of Fluid Mechanics*, Vol. 26, 1966, p. 163.
- ⁶Klineberg, J. and Steger, J., "On Laminar Boundary-Layer Separation," AIAA Paper 74-94, 1974.
- ⁷Anderson, D. A., Tannehill, J. C., and Pletcher, R. H., *Computational Fluid Mechanics and Heat Transfer*, Hemisphere, Washington, New York, London, 1984.
- ⁸Edwards, D. E. and Carter, J. E., "A Quasi-Simultaneous Finite Difference Approach for Strongly Interacting Flow," Paper presented at Symposium on Numerical and Physical Aspects of Aerodynamic Flows, Jan. 1985.
- ⁹Halim, A. and Hafez, M., "Calculation of Separation Bubbles Using Boundary-Layer-Type Equations—Part I and II," AIAA Paper 84-1585, 1984.
- ¹⁰Inoue, O., "Separated Boundary Layer Flows with High Reynolds Numbers," *Lecture Notes in Physics*, Vol. 141, 1981, p. 224.
- ¹¹Hoffman, G. H., "Comparison of Parabolized Vorticity and Navier-Stokes Solutions in a Mildly Nonorthogonal Coordinate System," Pennsylvania State University, University Park, Rept. TM 82-72, 1982.
- ¹²Smith, F. T., "The High Reynolds Number Theory of Laminar Flow," *IMA Journal of Applied Mathematics*, Vol. 28, 1982, p. 207.
- ¹³Cheng, H. K. and Smith, F. T., "The Influence of Airfoil Thickness and Reynolds Number on Separation," *Zeitschrift für Angewandte Mathematik und Physik*, Vol. 30, 1982, p. 151.
- ¹⁴Cheng, H. K., "The Laminar Airfoil Beyond Trailing-Edge Stall, Part II," Paper presented at Third Symposium on Numerical and Physical Aspects of Aerodynamic Flows, Jan. 1985.
- ¹⁵Roache, P. J., "Scaling of High Reynolds Number Weakly Separated Flows," Paper presented at Third Symposium on Numerical and Physical Aspects of Aerodynamic Flows, Jan. 1981.
- ¹⁶Thompson, J. F., Thames, F. C., and Mastin, C. W., "Automatic Numerical Generation of Body Fitted Curvilinear Coordinate System for Fields Containing Any Number of Arbitrary Two-Dimensional Bodies," *Journal of Computational Physics*, Vol. 15, 1974, p. 299.
- ¹⁷Napolitano, M. and Walters, R. W., "An Incremental Block-Line-Gauss-Seidel Method for the Navier-Stokes Equations," *AIAA Journal*, Vol. 26, May 1986, pp. 770-776.
- ¹⁸Davis, R. T., "Numerical Solutions of the Navier-Stokes Equations for Symmetric Laminar Incompressible Flow Past a Parabola," *Journal of Fluid Mechanics*, Vol. 51, 1972, p. 417.
- ¹⁹Beam, R. M. and Warming, R. F., "An Implicit Factored Scheme for the Compressible Navier-Stokes Equations," *AIAA Journal*, Vol. 16, April 1978, p. 393.